

The cosmological lithium problem outside the Galaxy: the Sagittarius globular cluster M54[★]

A. Mucciarelli,^{1†} M. Salaris,² P. Bonifacio,³ L. Monaco⁴ and S. Villanova⁵

¹Dipartimento di Fisica & Astronomia, Università degli Studi di Bologna, Viale Berti Pichat, 6/2, I - 40127 Bologna, Italy

²Astrophysics Research Institute, Liverpool John Moores University, IC2, 146 Brownlow Hill, Liverpool L3 5RF, UK

³GEPI, Observatoire de Paris, CNRS, Univ. Paris Diderot, 92125 Meudon Cedex, France

⁴European Southern Observatory, Casilla 19001, Santiago, Chile

⁵Universidad de Concepcion, Casilla 160-C, Concepcion, Chile

Accepted 2014 July 28. Received 2014 July 5; in original form 2014 May 10

ABSTRACT

The cosmological Li problem is the observed discrepancy between Li abundance ($A(\text{Li})$) measured in Galactic dwarf, old and metal-poor stars (traditionally assumed to be equal to the initial value $A(\text{Li})_0$), and that predicted by standard big bang nucleosynthesis (BBN) calculations ($A(\text{Li})_{\text{BBN}}$). Here, we attack the Li problem by considering an alternative diagnostic, namely the surface Li abundance of red giant branch stars that in a colour–magnitude diagram populate the region between the completion of the first dredge-up and the red giant branch bump. We obtained high-resolution spectra with the FLAMES facility at the Very Large Telescope for a sample of red giants in the globular cluster M54, belonging to the Sagittarius dwarf galaxy. We obtain $A(\text{Li}) = 0.93 \pm 0.11$ dex, translating – after taking into account the dilution due to the dredge-up – to initial abundances ($A(\text{Li})_0$) in the range 2.35–2.29 dex, depending on whether or not atomic diffusion is considered. This is the first measurement of Li in the Sagittarius galaxy and the more distant estimate of $A(\text{Li})_0$ in old stars obtained so far. The $A(\text{Li})_0$ estimated in M54 is lower by ~ 0.35 dex than $A(\text{Li})_{\text{BBN}}$, hence incompatible at a level of $\sim 3\sigma$. Our result shows that this discrepancy is a universal problem concerning both the Milky Way and extragalactic systems. Either modifications of BBN calculations, or a combination of atomic diffusion plus a suitably tuned additional mixing during the main sequence, need to be invoked to solve the discrepancy.

Key words: stars: abundances – stars: atmospheres – stars: Population II – globular clusters: individual: M54.

1 INTRODUCTION

Lithium, together with hydrogen and helium, is produced in the first minutes after the big bang, and its primordial abundance is a function of the cosmological density of baryons. An estimate of this primordial Li abundance provides therefore an important test for current standard cosmological models. Spite & Spite (1982) first discovered that dwarf (main sequence, turn-off or subgiants), Population II stars with effective temperatures (T_{eff}) between ~ 5700 and ~ 6300 K and $[\text{Fe}/\text{H}] < -1.4$ dex share the same Li abundance, the so-called *Spite Plateau*. The existence of a narrow Li *Plateau* has been confirmed by three decades of observations (see e.g. Rebolo, Beckman & Molaro 1988; Bonifacio & Molaro 1997; Asplund et al. 2006; Bonifacio et al. 2007); when considering stellar evolution

calculations that include only convection as element transport, this plateau corresponds to the primordial Li abundance in the Galactic halo, that is usually identified as the Li abundance produced during the big bang nucleosynthesis ($A(\text{Li})_{\text{BBN}}$). The measured Li abundance in *Spite Plateau* dwarfs is in the range $A(\text{Li})^1 = 2.1\text{--}2.3$ dex, depending on the adopted T_{eff} scale.

On the other hand, the very accurate determination of the baryonic density obtained from the *Wilkinson Microwave Anisotropy Probe* (Spergel et al. 2007; Hinshaw et al. 2013) and *Planck* (Planck collaboration 2013) satellites, coupled with the BBN standard model, has allowed us to calculate $A(\text{Li})_{\text{BBN}}$. The derived values (2.72 ± 0.06 dex; Cyburt, Fields & Olive 2008, and 2.69 ± 0.04 ; Coc et al. 2013) are significantly higher, about a factor of 3, than that measured in dwarf stars.

[★] Based on data taken at the ESO, within the observing program 089.D-0341.

[†] E-mail: alessio.mucciarelli2@unibo.it

¹ $A(\text{Li}) = \log \frac{n(\text{Li})}{n(\text{H})} + 12.00$

A first potential solution to this discrepancy between $A(\text{Li})_{\text{BBN}}$ from BBN calculations and *Spite Plateau* measurements (denoted here as the *cosmological Li problem*) envisages the inclusion of atomic diffusion in stellar model calculations. Atomic diffusion is a physical process that can be modelled parameter-free from first principles, it is efficient in the Sun (see e.g. Bahcall et al. 1997), and can deplete efficiently the surface abundance of Li in metal-poor main-sequence stars. However, because the degree of depletion increases with effective temperature (and decreasing metallicity), it is not possible to reproduce the observed plateau-like abundance trend (see e.g. Richard, Michaud & Richer 2005, and references therein) if atomic diffusion is fully efficient in objects populating the *Spite Plateau*, see e.g. fig. 3 in Mucciarelli et al. (2011).

Recent proposed solutions to the *cosmological Li problem* are as follows:

(i) the combined effect of atomic diffusion and some competing additional mixing – necessary to preserve the existence of an abundance *plateau* – whose combined effect decreases the Li abundance in the atmospheres of dwarf stars (Richard et al. 2005; Korn et al. 2006); (ii) inadequacies of the BBN model used to calculate $A(\text{Li})_{\text{BBN}}$ (see e.g. Iocco et al. 2009); (iii) an Li depletion driven by Population III stars during the early Galaxy evolution (Piau et al. 2006).

Mucciarelli, Salaris & Bonifacio (2012, MSB12) proposed an alternative/complementary route to investigate the initial Li abundance in Population II stars ($A(\text{Li})_0$), by measuring the surface Li abundance in lower red giant branch (RGB) stars. These stars are located between the completion of the first dredge-up (FDU, where Li-free material is mixed to the surface by convection) and the luminosity level of the RGB bump (where an additional mixing episode occurs; see Gratton et al. 2000). These giants are characterized by a constant Li abundance (at fixed $[\text{Fe}/\text{H}]$), drawing a *Plateau* that mirrors the *Spite Plateau* but at a lower abundance ($A(\text{Li}) \sim 0.9\text{--}1.0$ dex). The amount of Li depletion due to dilution after the FDU can be predicted easily by stellar models. Lower RGB stars are therefore a powerful alternative diagnostic of $A(\text{Li})_0$, mainly because the derived value is very weakly affected by atomic diffusion during the previous main-sequence phase. This means that it is possible to put strong constraints on $A(\text{Li})_0$, irrespective of whether atomic diffusion is effective or not, and assess whether additional processes – within the stars, or during the BBN, or during Galaxy formation – need to be invoked to match the BBN calculations of Li abundances. Moreover, lower RGB stars also enable to investigate $A(\text{Li})_0$ in stars more distant than those usually observed for *Spite Plateau* studies.

In this paper, we exploit this new diagnostic with the aim to study $A(\text{Li})_0$ in M54, a massive globular cluster (GC) immersed in the nucleus of the Sagittarius (Sgr) dwarf galaxy (Monaco et al. 2005; Bellazzini et al. 2008). The dwarf stars in M54 and Sgr are too faint ($V \sim 22$) to be observed, thus the study of lower RGB stars represents the only possible route to infer $A(\text{Li})_0$ in this galaxy. Section 2 describes the spectroscopic observations, followed in Section 3 by the determination of the Li abundances and the constraints on $A(\text{Li})_0$ for M54 stars, and is followed by a discussion of the results and conclusions.

2 OBSERVATIONS

High-resolution spectra of lower RGB stars in M54 have been secured with the multi-object spectrograph FLAMES (Pasquini et al. 2002) at the ESO Very Large Telescope, in the GIRAFFE/MEDUSA mode. The observations have been performed with the setups HR12 (to sample the Na D lines, with a resolution of 18 700) and HR15N

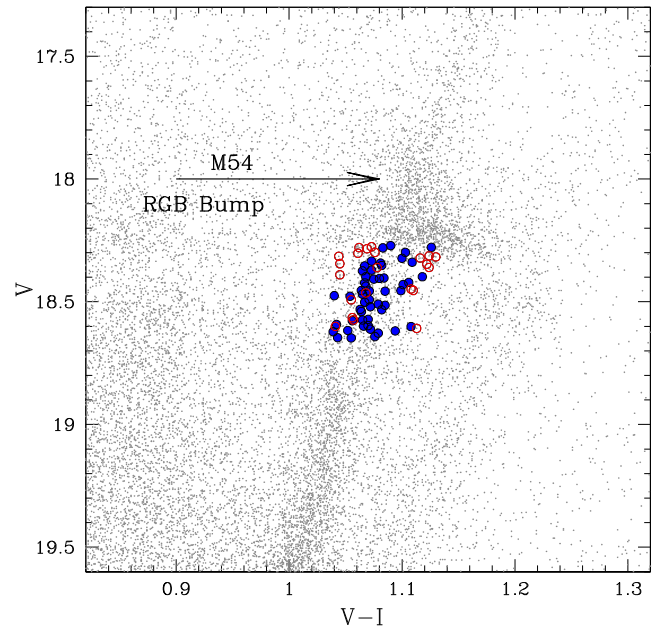


Figure 1. Colour–magnitude diagram of M54+Sgr that displays also the observed targets. Blue filled circles denote the member stars of M54, red empty circles the Sgr field stars.

(to sample the Li doublet at 6707 Å, with a resolution of 17 000). The same target configuration has been used for both gratings and each target has been observed for a total time of 26 and 4 h, for HR15N and HR12, respectively.

The targets have been selected from ACS@*HST* photometry (Siegel et al. 2007) for the central region and from WFI@ESO photometry (Monaco et al. 2002) for the outermost region. 85 stars have been selected along the RGB of M54 in the magnitude range $V = 18.3\text{--}18.6$, being its RGB bump at $V \sim 18$, according to the RGB luminosity function. We excluded the 0.2 magnitudes below the RGB bump to minimize the contamination from the Sgr He-Clump stars. Fig. 1 shows the colour–magnitude diagram of M54 with marked the observed targets (red and blue points). The signal-to-noise (SNR) ratio per pixel around the Li doublet ranges from ~ 30 to ~ 50 , with an average value of 42.

The spectra have been processed with the GIRAFFE data reduction pipeline, including bias-subtraction, flat-fielding, wavelength calibration, spectral extraction.² Radial velocities have been measured with DAOSPEC (Stetson & Pancino 2008) by using ~ 15 metallic lines. 11 targets have been discarded because they are clearly Galactic interlopers, with radial velocities between -105 and $+60$ km s^{−1} (see fig. 8 in Bellazzini et al. 2008). Finally, our sample includes a total of 74 candidate member stars of M54 (their main information is listed in Table 1).

3 CHEMICAL ANALYSIS

Values of T_{eff} have been derived from the $(V - I)_0$ colour by means of the calibration by Alonso, Arribas & Martínez-Roger (1999), adopting the colour excess $E(B - V) = 0.14$ mag (Layden & Sarajedini 2000) and the extinction coefficients by McCall (2004). Surface gravities have been calculated from the Stefan–Boltzmann relation assuming the photometric T_{eff} , the bolometric corrections by Alonso

² <https://www.eso.org/sci/software/pipelines/>

Table 1. Identification numbers, coordinates, effective temperature, surface gravity, radial velocity, [Fe/H] and [Na/Fe] abundances. Final flag indicates the membership to M54 or to Sgr.

ID	RA (J2000)	Dec. (J2000)	T_{eff} (K)	$\log g$	RV (km s ⁻¹)	[Fe/H] (dex)	[Na/Fe] (dex)	Flag
6750	283.794 8303	-30.499 0501	5010	2.50	130.5	-1.75	-0.56	M54
7590	283.793 3655	-30.493 5970	5010	2.51	140.9	-1.65	0.38	M54
12291	283.786 4380	-30.501 9646	4987	2.47	151.8	-2.00	-0.40	M54
21190	283.776 9165	-30.505 2319	4921	2.40	135.7	-1.74	0.16	M54
51661	283.753 0823	-30.503 7270	4916	2.41	148.5	-0.34	-0.48	Sgr
53985	283.751 4343	-30.493 7611	4936	2.37	149.1	-1.74	0.09	M54
56686	283.748 6572	-30.504 5719	5018	2.45	141.6	-1.42	0.25	M54
65022	283.739 1968	-30.504 7073	5046	2.52	149.3	-1.24	0.46	Sgr
69373	283.733 3679	-30.493 2117	4977	2.37	144.5	-1.56	-0.21	M54
75429	283.795 0134	-30.484 8213	5028	2.50	149.3	-1.58	-0.19	M54
86412	283.784 7900	-30.492 2523	5079	2.56	146.1	-1.95	0.58	M54
91967	283.781 4636	-30.480 0529	4975	2.42	142.1	-1.86	0.47	M54
121249	283.768 5242	-30.491 7202	4873	2.32	153.5	-1.86	-0.07	M54
141357	283.761 9019	-30.491 5009	5023	2.51	146.1	-1.87	0.25	M54
155785	283.757 5684	-30.485 2924	5023	2.43	141.1	-1.66	0.26	M54
201571	283.727 6917	-30.491 5905	5015	2.46	144.4	-0.96	0.04	Sgr
208256	283.791 5344	-30.473 9513	5082	2.54	143.7	-1.93	0.16	M54
216867	283.784 1797	-30.468 4467	5007	2.47	142.7	-1.79	0.23	M54
231677	283.775 3906	-30.477 8271	5048	2.55	136.0	-1.70	-0.22	M54
235280	283.773 8342	-30.473 5279	5056	2.54	147.3	-1.66	0.53	M54
279832	283.757 5073	-30.466 6042	5090	2.56	148.6	-1.79	0.58	M54
299467	283.748 1689	-30.472 8985	4960	2.36	149.6	-1.72	0.27	M54
304691	283.745 0256	-30.466 5394	5005	2.48	139.0	-1.31	0.18	M54
315861	283.735 9009	-30.474 5407	5025	2.50	140.6	-1.60	-0.07	M54
335718	283.780 0903	-30.457 4833	5005	2.52	150.1	-1.67	-0.28	M54
340297	283.775 4211	-30.457 0541	4980	2.47	136.6	-1.63	-0.14	M54
342644	283.773 2849	-30.454 3114	5018	2.42	142.6	-1.62	0.10	M54
348795	283.768 1274	-30.456 7890	5002	2.41	149.6	-1.73	0.30	M54
356601	283.761 4441	-30.463 7871	5025	2.46	145.1	-1.59	0.53	M54
358028	283.760 7117	-30.451 4027	4928	2.36	144.2	-1.66	0.01	M54
359389	283.759 3689	-30.457 3898	5051	2.48	147.2	-1.37	-0.14	M54
379953	283.737 5183	-30.462 4958	5048	2.49	137.9	-0.90	-0.14	Sgr
1031659	283.792 0227	-30.427 7306	5002	2.38	161.6	-1.15	-0.07	Sgr
1031785	283.745 2393	-30.513 5555	5030	2.40	136.6	-1.12	0.03	Sgr
1032003	283.847 1985	-30.334 1923	5012	2.39	140.1	-0.71	0.21	Sgr
1032576	283.768 3716	-30.401 1650	4995	2.39	177.8	-1.25	-0.29	Sgr
1032677	283.671 6309	-30.329 7195	5033	2.41	151.0	-0.86	-0.15	Sgr
1033129	283.585 7239	-30.453 4187	4878	2.34	150.6	-0.79	-	Sgr
1033207	283.730 9570	-30.509 3040	5077	2.43	137.6	-0.90	-0.50	Sgr
1033253	283.712 6770	-30.371 6583	4864	2.33	145.8	-0.88	-0.71	Sgr
1033431	283.760 8337	-30.602 5276	4897	2.35	165.9	-1.14	-0.05	Sgr
1033794	283.833 5571	-30.608 6063	4953	2.38	142.7	-	-	Sgr
1033808	283.669 7998	-30.569 1261	4975	2.39	144.7	-0.91	0.03	Sgr
1034001	283.736 9385	-30.434 7324	4914	2.37	146.6	-1.68	-0.48	M54
1034068	283.705 4138	-30.494 2036	4982	2.40	141.2	-1.67	0.54	M54
1034166	283.614 7766	-30.510 9158	5074	2.44	102.8	-0.95	0.44	Sgr
1034215	283.625 6104	-30.464 0865	4883	2.35	162.6	-0.56	-0.49	Sgr
1034363	283.725 0061	-30.444 3989	4980	2.40	146.5	-1.48	0.24	M54
1034592	283.838 6841	-30.481 5445	4878	2.36	159.7	-0.47	-0.68	Sgr
1034628	283.879 5471	-30.353 9162	4990	2.41	144.3	-1.00	-0.62	Sgr
1034807	283.722 0154	-30.337 0037	4627	2.32	147.1	-0.46	-0.49	Sgr
1034871	283.698 3032	-30.493 2556	5002	2.42	148.2	-1.74	0.77	M54
1035051	283.589 6912	-30.457 9124	4975	2.41	149.7	-0.94	-0.98	Sgr
1035061	283.894 8059	-30.482 7633	4678	2.36	155.8	-0.83	-0.55	Sgr
1035450	283.779 2969	-30.521 8792	5074	2.46	142.8	-0.94	0.33	Sgr
1035614	283.696 5637	-30.472 0631	4706	2.38	141.5	-0.55	-0.71	Sgr
1035639	283.936 3708	-30.359 3540	4777	2.42	138.1	-0.55	-	Sgr
1035659	283.893 7683	-30.523 1647	5015	2.44	143.6	-1.77	-0.15	M54
1035689	283.664 6118	-30.408 3195	4892	2.38	125.6	-1.75	0.24	M54
1035733	283.687 1338	-30.567 7834	5074	2.46	140.8	-0.90	0.23	Sgr

Table 1 – continued

ID	RA (J2000)	Dec. (J2000)	T_{eff} (K)	$\log g$	RV (km s ⁻¹)	[Fe/H] (dex)	[Na/Fe] (dex)	Flag
1035834	283.723 9990	-30.456 3236	4985	2.43	141.3	-1.55	-0.27	M54
1035938	283.753 6316	-30.447 6051	4997	2.43	123.1	-1.74	-0.32	M54
1035965	283.638 9771	-30.507 7534	4670	2.36	147.7	-0.39	-	Sgr
1036018	283.700 1953	-30.576 0975	4738	2.40	140.0	0.07	-0.40	Sgr
1036558	283.718 4753	-30.478 2505	4933	2.41	138.1	-1.66	-0.03	M54
1036741	283.799 3469	-30.491 6420	5015	2.45	137.5	-1.66	0.06	M54
1036890	283.854 3091	-30.514 4444	4716	2.40	116.0	-1.04	-0.24	Sgr
1037256	283.981 7505	-30.482 2559	4660	2.38	146.0	-0.56	-0.43	Sgr
1037298	283.744 5984	-30.518 5242	4911	2.41	158.1	-0.96	0.15	Sgr
1037347	283.586 8835	-30.534 3914	4747	2.43	151.9	0.24	0.15	Sgr
1037357	283.728 7598	-30.394 1364	4938	2.42	144.0	-1.55	0.27	M54
1037383	283.758 2397	-30.447 4907	5007	2.46	151.0	-1.58	0.38	M54
1037405	283.802 9785	-30.609 7832	4972	2.44	145.7	-1.40	-	M54
1037499	283.902 3132	-30.580 4310	5082	2.49	132.9	-1.15	-	Sgr
1037755	283.806 8848	-30.476 6140	5023	2.47	143.1	-1.50	0.27	M54
1037842	283.652 2827	-30.411 4075	4773	2.45	149.4	-0.84	-0.16	Sgr
1037956	283.788 3301	-30.517 6754	5087	2.50	129.4	-1.62	0.51	M54
1038371	283.747 3450	-30.421 9704	4687	2.41	130.4	-0.82	-0.78	Sgr
1038827	283.727 1729	-30.461 4105	5018	2.48	145.7	-1.64	0.07	M54
1038900	283.951 9348	-30.577 0645	4682	2.41	143.3	-0.30	-0.47	Sgr
1039247	283.729 3701	-30.535 1334	4972	2.46	146.1	-1.52	0.34	M54
1039380	283.641 6626	-30.418 8614	4764	2.46	123.5	-0.65	-0.26	Sgr
1039482	283.996 3989	-30.481 8535	4782	2.47	138.4	-0.64	-	Sgr
1039645	283.758 6670	-30.577 2209	4800	2.48	133.7	-0.27	-0.47	Sgr
1040277	283.887 6648	-30.428 6728	4807	2.49	142.9	-0.61	-0.49	Sgr
1040695	283.893 5852	-30.612 9131	4775	2.48	159.6	-0.10	-	Sgr
1040996	283.720 1233	-30.587 4443	4716	2.45	143.2	-0.47	-0.87	Sgr
1041212	283.724 1211	-30.536 1309	5043	2.52	144.3	-1.03	-0.09	Sgr
1041214	284.001 4343	-30.513 8874	4816	2.51	142.7	-0.06	-	Sgr
1041231	283.781 4636	-30.655 7369	4682	2.44	140.2	-	-	Sgr
1041308	283.800 0793	-30.439 9662	5046	2.52	149.8	-1.75	0.06	M54
1041392	283.759 6741	-30.637 0296	4798	2.50	160.3	0.52	-0.78	Sgr
1041896	283.880 8899	-30.447 2752	4718	2.47	133.9	-0.66	-0.52	Sgr
1041905	283.852 5391	-30.491 7564	4784	2.50	146.9	-0.61	-0.56	Sgr
1042086	283.804 7180	-30.466 4555	5020	2.52	142.2	-1.99	0.59	M54
1042102	283.725 3723	-30.482 7061	5085	2.55	143.9	-0.92	-	Sgr
1042123	283.768 0359	-30.439 7469	4916	2.47	141.1	-1.77	-0.11	M54
1042352	283.645 2942	-30.479 3129	4904	2.47	165.3	-1.25	-0.03	Sgr
1042739	283.741 9739	-30.423 4066	4950	2.49	146.3	-1.47	-0.22	M54
1043020	283.769 7144	-30.527 8034	4987	2.52	141.2	-1.87	-	M54
1043447	283.713 7451	-30.328 0296	4995	2.52	154.8	-1.51	-0.21	M54

et al. (1999) and the distance modulus $(m - M)_0 = 17.10$ mag (Monaco et al. 2004). We assumed a mass of $0.8 M_{\odot}$, according to a BaSTI isochrone (Pietrinferni et al. 2006) with 12 Gyr, $Z = 0.0003$ and α -enhanced chemical mixture. A microturbulent velocity $v_{\text{turb}} = 1.5$ km s⁻¹ has been assumed for all the targets, taking the median value of v_{turb} of the lower RGB stars analysed by MSB12.

Fe and Na abundances have been derived from the line equivalent widths (EWs) by using the code GALA (Mucciarelli et al. 2013), coupled with ATLAS9 model atmospheres. Fe abundances have been obtained from the measure of ~ 10 – 15 Fe I lines, while Na abundances from the Na D lines at 5889–5895 Å. EWs of Fe lines have been measured with DAOSPEC (Stetson & Pancino 2008), while those of the Na lines by using IRAF assuming a Voigt profile. Non-local thermodynamical equilibrium (NLTE) corrections for the Na abundances are from Gratton et al. (1999). The recent NLTE calculations by Lind et al. (2011) provide $[\text{Na/Fe}]_{\text{NLTE}}$ lower by about 0.2–0.3 dex; however, in the following we refer to the abundances obtained

with the corrections by Gratton et al. (1999) to allow a direct comparison with Carretta et al. (2010) that measured Na abundances in 76 stars of M54. Fig. 2 shows the metallicity distribution of the 74 candidate M54 member stars, ranging from $[\text{Fe/H}] = -2.0$ up to -0.34 dex, with a main peak at ~ -1.7 dex and a second peak at ~ -0.9 dex.

We consider as members of M54: (i) stars with radial velocity between 100 and 170 km s⁻¹, (Bellazzini et al. 2008), and (ii) stars with $[\text{Fe/H}] < -1.3$ dex, in order to exclude the stars of the second peak observed in the metallicity distribution, likely belonging to the Sgr field (note that the metallicity distributions of M54 by Bellazzini et al. 2008 and Carretta et al. 2010 are both broad but they do not show evidence of bimodality). Finally, 51 targets are considered as *bona fide* M54 member stars. These stars are shown as blue circles in Fig. 1 and as the shaded histogram in Fig. 2. The mean iron content is $[\text{Fe/H}] = -1.67 \pm 0.02$ dex ($\sigma = 0.15$ dex), compatible with those derived by Bellazzini et al. (2008) and Carretta et al. (2010). The M54 member stars show a wide range of $[\text{Na/Fe}]$, between -0.56

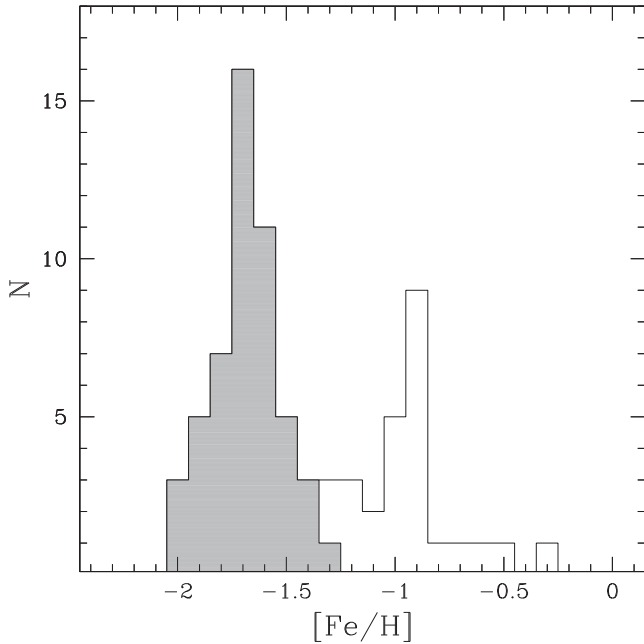


Figure 2. $[\text{Fe}/\text{H}]$ distribution for the RGB stars of M54. The grey shaded histogram includes the targets considered as members of M54, according to radial velocity and iron content.

and $+0.77$ dex, with an average value $[\text{Na}/\text{Fe}] = +0.11 \pm 0.04$ dex ($\sigma = 0.31$ dex), fully consistent with the results by Carretta et al. (2010).

The Li abundances have been derived from the Li resonance doublet at ~ 6707 Å, by comparing the observed spectra with a grid of synthetic spectra, calculated with the code *SYNTH* (Sbordone et al. 2004). NLTE corrections are from Lind et al. (2008). The uncertainty in the fitting procedure has been estimated with Monte Carlo simulations performed by analysing synthetic spectra with the injection of Poissonian noise. Also, we included in the total error budget of the Li abundance the impact of the uncertainties in T_{eff} , the other parameters having a negligible impact on $A(\text{Li})$. Because of the weakness of the Li doublet ($\text{EW} \sim 13$ mÅ), at the SNR of our spectra it cannot be properly measured in each individual spectrum. Thus, we grouped together all the spectra of the stars considered as members of M54, obtaining an average spectrum with $\text{SNR} \sim 300$ and assuming the average atmospheric parameters of the sample, namely $T_{\text{eff}} = 4995$ K and $\log g = 2.46$. These stars are located in a narrow region of the colour–magnitude diagram, legitimating this procedure. In particular, T_{eff} is the most critical parameter for the Li abundance estimate, whereas $\log g$ and v_{turb} have a negligible impact. The 51 cluster members cover a T_{eff} range between 4873 and 5090 K, with a mean equal to 4995 K ($\sigma = 48$ K), and a median value of 5005 K with an interquartile range of 51 K. Fig. 3 shows the Li doublet observed in the average spectrum, with superimposed the best-fitting synthetic spectrum (red solid line) and two synthetic spectra calculated with ± 0.2 dex with respect to the best-fitting abundance (red dashed lines).

The final derived Li abundance is $A(\text{Li})_{\text{NLTE}} = 0.93 \pm 0.03 \pm 0.11$ dex (where the first error bar is the internal error as derived by the Monte Carlo simulations, and the second one is due to the T_{eff} uncertainty). For consistency with MSB12, we checked also $A(\text{Li})_{\text{NLTE}}$ obtained with the NLTE corrections by Carlsson et al. (1994), that lead to an increase of the final abundance by 0.08 dex, thus providing $A(\text{Li})_{\text{NLTE}} = 1.01$ dex. The choice of the NLTE

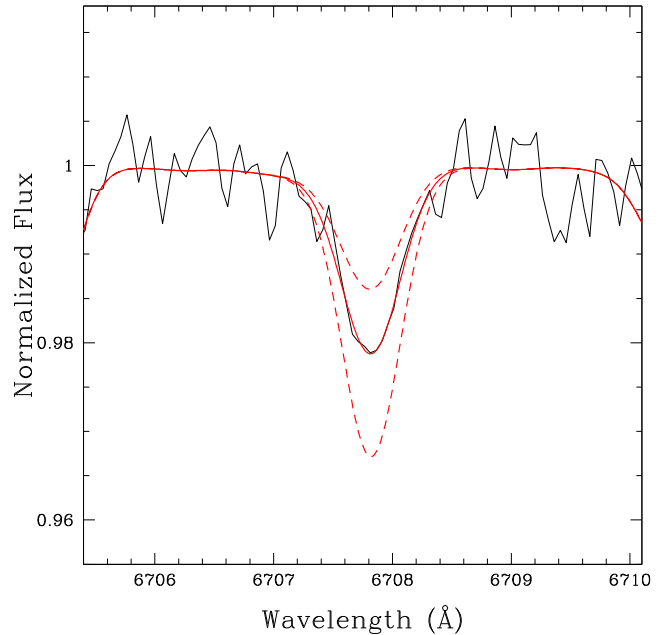


Figure 3. The observed Li doublet of the average spectrum obtained by combining all 51 targets that are members of M54. The red solid line is the best-fitting synthetic spectrum, whilst the red dashed lines display the synthetic spectra calculated with ± 0.2 dex variations with respect to the best-fitting abundance.

corrections has obviously a small impact of the final $A(\text{Li})$ value and does not change drastically our conclusions.

3.1 Checks about the average spectrum

To assess the stability of our results against the way we group the spectra, we have performed a number of sanity checks. In these tests, we divided the cluster sample into two bins, according to:

- (a) $[\text{Fe}/\text{H}]$; the two groups include stars with $[\text{Fe}/\text{H}]$ lower and higher than the median value of $[\text{Fe}/\text{H}]$ ($[\text{Fe}/\text{H}] = -1.67$, see Fig. 2), respectively;
- (b) T_{eff} ; the boundary between the two groups is the median T_{eff} ;
- (c) magnitude; the two groups include stars fainter and brighter than the median V-band magnitude ($V = 18.45$), respectively;
- (d) $[\text{Na}/\text{Fe}]$; the boundary between the two groups is the median value of the $[\text{Na}/\text{Fe}]_{\text{NLTE}}$ distribution ($[\text{Na}/\text{Fe}]_{\text{NLTE}} = +0.16$ dex).

For all these cases, we found $A(\text{Li})_{\text{NLTE}}$ compatible within the uncertainties with the value obtained with the average spectrum of the whole cluster targets, as shown by Fig. 4. The largest difference (0.08 dex, still compatible within 1σ with the original value), is found when we group together spectra with V-band magnitude fainter than $V = 18.45$, because they have the lowest SNR. In light of these results, we can conclude that no significant biases related to the grouping of the target spectra affect our Li abundance estimate.

Another point to discuss here concerns the use of a single value of the NLTE correction computed for the average atmospheric parameters of the whole sample. To this purpose, we notice that the variation of the NLTE corrections in the parameter space covered by our targets is small: in particular, at fixed T_{eff} $\log g$ the corrections vary by ~ 0.03 – 0.04 dex between the minimum and maximum $[\text{Fe}/\text{H}]$ of the metallicity distribution, while at fixed metallicity, the corrections change by ~ 0.03 dex between the minimum and

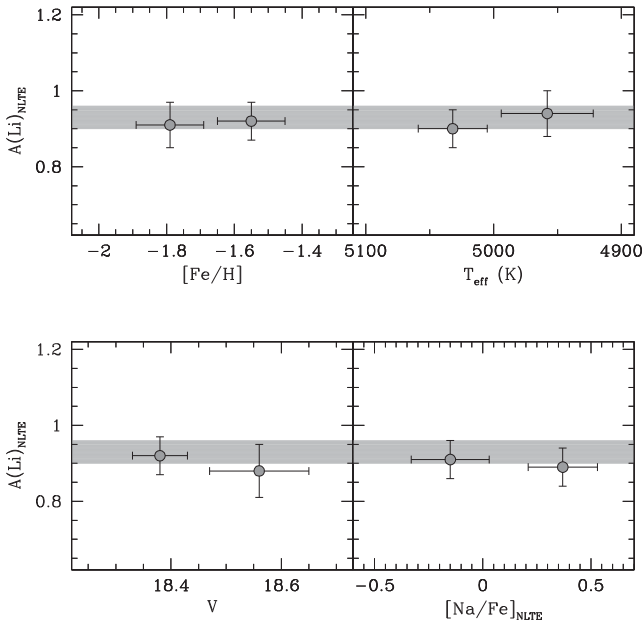


Figure 4. $A(\text{Li})_{\text{NLTE}}$ values (dark grey circles) obtained by grouping the sample of M54 member stars into two average spectra according to the median value of [Fe/H] (left-upper panel), T_{eff} (right-upper panel), V-band magnitude (left-lower panel) and [Na/Fe] (right-lower panel). Abundance error bars include only the internal uncertainty from Monte Carlo simulations. Error bars along the x-axis denote the 1σ spread around the mean value of each quantity. The shaded grey area in each panel denotes the $\pm 1\sigma$ range with respect to the $A(\text{Li})_{\text{NLTE}}$ obtained from the average spectrum of the whole M54 sample.

maximum T_{eff} . To investigate more rigorously this effect, we simulated a spectrum with the following procedure: (1) for each individual member star, a synthetic spectrum has been calculated with the appropriate atmospheric parameters and iron abundance, imposing a Li abundance $A(\text{Li})_{\text{NLTE}} = 0.93$ dex (to take into account the proper NLTE correction of each star); (2) the spectra have been rescaled according to the relative differences in magnitude; (3) Poissonian noise has been injected in each synthetic spectrum to reproduce the measured SNR of the observed counterpart; (4) all these synthetic spectra have been co-added as done with the observed sample.

The entire procedure is repeated to obtain a sample of 1000 average spectra that has been analysed as done with the observed stars. The derived $A(\text{Li})_{\text{NLTE}}$ distribution (assuming a single value of the NLTE correction) displays a mean value equal to 0.95 dex with a dispersion of 0.04 dex. This simulation confirms that star-to-star variations of the NLTE corrections are only a second order effect and do not affect substantially the abundance derived from the average spectrum.

3.2 Lithium abundance and chemical anomalies in GCs

It is well established that individual GCs harbour subpopulations characterized by different abundances of light elements, like Na and O (see e.g. Gratton, Carretta & Bragaglia 2012). In principle, these so-called *second-generation* stars, characterized by high values of [Na/Fe] and low values of [O/Fe], should display lower Li abundances, because they are predicted to be born from gas diluted with Li-poor material coming from asymptotic giant branch or fast-rotating massive stars. Given that the thermonuclear reactions able to produce the observed chemical patterns occur at temperatures larger than $\sim 10^7$ K, while Li is destroyed at lower

temperatures ($\sim 2.5 \times 10^6$ K), second-generation stars should exhibit lower abundances of Li compared to first-generation stars. In particular, Li depletions, Li–O correlations and Li–Na anticorrelations are expected within individual clusters. Empirically, clear Li–O correlations have been detected in NGC 6752 (Shen et al. 2010) and 47 Tuc (Dobrovolskas et al. 2014). Three Na-rich stars (thus belonging to the second cluster generation) with low Li abundance ($A(\text{Li}) < 2.0$ dex) have been detected in NGC 6397 (Lind et al. 2009), while most of the observed stars display a uniform Li (compatible with the *Spite Plateau*) but a large range of Na, suggesting that Li depletion is negligible for the second-generation stars of this cluster. M4 displays a very small (if any) intrinsic Li dispersion, without correlation between O and Li abundance (Mucciarelli et al. 2011) and with a weak Li–Na anticorrelation (Monaco et al. 2012). Lower RGB stars in M12 share all the same Li content, whilst there is a spread of Li in M5, but no statistically significant Li–O correlations and Li–Na anticorrelations (D’Orazi et al. 2014).

We have checked whether potential systematic differences between $A(\text{Li})$ of first- and second-generation stars in M54 can affect our conclusions. As discussed in Section 3.1, we divided the sample of M54 stars into two groups, according to their [Na/Fe] abundances, adopting as boundary the median value of the [Na/Fe] distribution (+0.16 dex). The derived average spectra show a very similar Li content, $A(\text{Li})_{\text{NLTE}} = 0.91 \pm 0.05$ and 0.89 ± 0.05 dex for the Na-poor and Na-rich groups, respectively, consistent with the value for the whole sample (see left-bottom panel in Fig. 4). Note that systematic differences in the Li content between the two samples smaller than ~ 0.1 dex (compatible, for instance, with those observed by Monaco et al. 2012 in M4) cannot be ruled out. However, such a small possible Li depletion in Na-rich stars of M54 does not change our conclusion about $A(\text{Li})_0$ in this cluster.

3.3 $A(\text{Li})_0$ in M54

To constrain the initial $A(\text{Li})_0$ in M54, we adopted the same procedure discussed in MSB12, by using the amount of Li depletion due to the FDU as predicted by stellar models (see their table 2). For a metallicity [Fe/H] = -1.67 dex, the predicted value is equal to 1.36 and 1.42 dex without and with atomic diffusion, respectively. As already discussed by MSB12, the amount of Li depletion along the RGB Plateau is marginally sensitive to the efficiency of the atomic diffusion that affects the dwarf stars much more strongly. We recall that M54 has an intrinsic iron dispersion (Carretta et al. 2010); however, the predicted Li depletion changes by ± 0.02 dex with respect to the values quoted above if we consider the minimum and maximum value of the cluster metallicity distribution, namely [Fe/H] = -2.0 and -1.3 dex. We can thus neglect the effect of the cluster metallicity spread.

The derived $A(\text{Li})_0$ in M54 is $A(\text{Li})_0 = 2.29 \pm 0.11$ dex (the error bar takes into account only the dominant effect of the uncertainty in T_{eff}) without diffusion and 2.35 ± 0.11 dex with fully efficient diffusion. When the NLTE corrections by Carlsson et al. (1994) are adopted, the range of $A(\text{Li})_0$ values is 2.37–2.43 dex.

4 DISCUSSION

This is the first study of the primordial Li abundance in M54 and, hence, in the Sgr galaxy. Also, it is the most distant measurement of $A(\text{Li})$ in old, metal-poor stars obtained so far, given that Li abundance determinations in dwarf stars are restricted to distances within ~ 8 kpc from the Sun (see the case of M92; Boesgaard et al. 1998; Bonifacio 2002). The use of lower RGB stars allows a giant

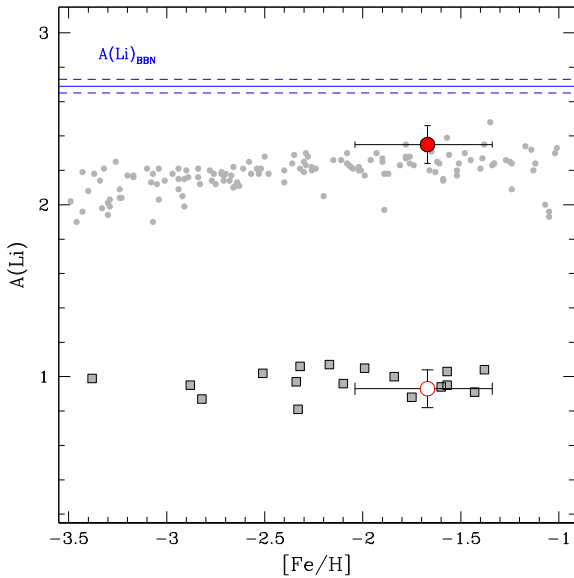


Figure 5. Li abundance as a function of $[\text{Fe}/\text{H}]$ for *Spite Plateau* and lower RGB field halo stars. Grey circles denote the dwarf sample (Bonifacio & Molaro 1997; Asplund et al. 2006; Aoki et al. 2009; Hosford et al. 2009; Melendez et al. 2010), and grey squares the lower RGB stars by MSB12. The empty red circle denotes the surface $A(\text{Li})$ in the lower RGB stars of M54, while the filled red circle displays the derived $A(\text{Li})_0$ assuming fully efficient atomic diffusion (the horizontal error bars associated with M54 data represent the range of $[\text{Fe}/\text{H}]$ covered by the cluster). The blue solid line denotes $A(\text{Li})_{\text{BBN}}$ (Coc et al. 2013), with the $\pm 1\sigma$ uncertainty denoted by blue dashed lines.

leap in the study of $A(\text{Li})_0$, pushing our investigation to ~ 25 kpc from the Sun and enlarging our perspective of the Li problem. This work demonstrates the potential of lower RGB stars to investigate $A(\text{Li})_0$ in stellar systems for which the observation of dwarf stars is precluded.

Fig. 5 compares our $A(\text{Li})$ and $A(\text{Li})_0$ for M54 stars (red empty and filled circle, respectively) to the results of Galactic field dwarf (grey circles) and lower RGB stars (grey squares). The value of $A(\text{Li})_{\text{BBN}}$ provided by Coc, Uzan & Vangioni (2013) is shown as reference. First of all, $A(\text{Li})$ measured in M54 red giants is in very good agreement with the results for the Galactic halo field (MSB12 found an average $A(\text{Li}) = 0.97$ with the same T_{eff} scale used for this study). Secondly, $A(\text{Li})_0$ inferred from the lower RGB of M54 has, as already said, a very small dependence on whether atomic diffusion is fully efficient or inhibited, and results to be on average ~ 0.04 – 0.10 dex higher than typical $A(\text{Li})$ values measured in dwarf stars, that are equal on average to $A(\text{Li}) \sim 2.25$ dex (see Fig. 5). Assuming the initial Li in M54 and the Galactic halo was the same, if atomic diffusion is fully efficient in *Spite Plateau* stars within the range of metallicities covered by M54 lower RGB stars, their surface Li abundances should be 0.4 – 0.7 dex lower than $A(\text{Li})_0$ (see e.g. fig. 3 in Mucciarelli et al. 2011).³

This means that either atomic diffusion is completely inhibited in halo field stars, and therefore the cosmological Li problem persists, or an additional element transport must be at work, burning during the main sequence more Li than predicted by models with diffusion

only. This route has been investigated in order to interpret the surface Li abundances measured in dwarf stars of Galactic GCs.

To this purpose, we first compare the results for M54 with measurements of $A(\text{Li})$ obtained for lower RGB stars in Galactic GCs that do not display a significant spread of Li. MSB12 determined $A(\text{Li}) = 1.00$ and $A(\text{Li}) = 0.92$ dex (both with ~ 0.10 dex error bars) for NGC 6397 ($[\text{Fe}/\text{H}] \sim -2.1$ dex) and M4 ($[\text{Fe}/\text{H}] \sim -1.1$ dex), respectively, using the same T_{eff} scale employed here. The same result has been found for lower RGB stars in M4 by Villanova & Geisler (2011). These values are well consistent with M54 result. The recent study by D’Orazi et al. (2014) found again a similar value, $A(\text{Li}) = 0.98$ dex, with an error bar of ~ 0.10 dex (using again the same T_{eff} scale of this work) for lower RGB stars in M12, another cluster with essentially no Li spread amongst lower RGB objects, and $[\text{Fe}/\text{H}]$ similar to M54.

Measurements of $A(\text{Li})$ in dwarfs stars have been performed in M92 (Boesgaard et al. 1998; Bonifacio 2002) NGC 6397 (Korn et al. 2006; Lind et al. 2008; Gonzalez Hernandez et al. 2009; Nordlander et al. 2012), NGC 6752 (Shen et al. 2010; Gruyters et al. 2013; Gruyters, Nordlander & Korn 2014), M4 (Mucciarelli et al. 2011; Monaco et al. 2012), 47 Tuc (D’Orazi et al. 2010; Dobrovolskas et al. 2014). To these GCs, we add also Omega Centauri (Monaco et al. 2010), a GC-like stellar system characterized by a wide range of metallicities and probably ages, and usually thought as the stripped core of a dwarf galaxy. All these works found that dwarf GC stars display on average a Li content compatible with the *Spite plateau*, confirming cosmological Li problem. The works on NGC 6397 and NGC 6752 by Gruyters et al. (2013) and Gruyters et al. (2014) have however addressed this issue by considering as potential solution, the combined effect of atomic diffusion and a hypothetical extra mixing process. In the following, we will consider the recent analysis by Gruyters et al. (2014) of Li abundances in NGC 6752, that has a $[\text{Fe}/\text{H}]$ very close to the mean value of M54. These authors followed the same procedures applied to infer $A(\text{Li})_0$ in NGC 6397 (see Nordlander et al. 2012 for the latest work on this cluster). They measured the abundances of Li, and additional metals like Mg, Ca, Ti and Fe, in cluster stars from the main-sequence turnoff to the lower RGB, and compared the abundance trends along these evolutionary phases with results from stellar model calculations by Richard, Michaud & Richer (2002). The observed trends could be matched only by models where the effect of diffusion was modulated by an additional mixing that in Richard et al. (2002) calculations is modelled as a diffusive process with diffusion coefficient D_T chosen as

$$D_T = 400 D_{\text{He}}(T_0) \left[\frac{\rho}{\rho(T_0)} \right]^{-3}, \quad (1)$$

where $D_{\text{He}}(T_0)$ is the atomic diffusion coefficient of He at a reference temperature T_0 , and $\rho(T_0)$ is the density of the stellar model at the same temperature. This is a somewhat ad hoc prescription, with the proportionality constant $400 D_{\text{He}}(T_0)$, and the steep dependence on ρ being essentially free parameters. A justification for the choice of the steep dependence on ρ stems from the need to restrict the efficiency of this mixing to a narrow region below the outer convection zone, as suggested by the solar beryllium abundance, believed to be essentially unaltered since the formation of the Solar system. The temperature T_0 is also a free parameter, that determines the depth where this diffusive mixing is most effective. It is important to remark that so far there has not been any attempt to test whether this mixing prescription can be associated to a well-established physical process like, i.e. rotationally induced mixing. Assuming that the prescription in equation (1) is realistic, Gruyters et al. (2014)

³ It is worth bearing in mind that a detailed comparison between $A(\text{Li})_0$ derived from lower RGB stars and the *Spite Plateau* depends also on the adopted T_{eff} scales and NLTE corrections; here, we simply take at face value the various estimates displayed in Fig. 5.

found that the free parameter T_0 has to be set to $\log(T_0) = 6.2$ to match the observed abundance trends for NGC 6752, resulting in $A(\text{Li})_0 = 2.53 \pm 0.10$, within less than 2σ of the BBN predictions.

To our purposes, it is relevant to notice that when $\log(T_0) = 6.2$, the lower RGB abundances of Richard et al. (2005) models decrease by ~ 0.1 dex compared to the case of pure diffusion, because during the main sequence additional Li is transported to the burning region by this extra mixing. If the same process and the same efficiency estimated for NGC 6752 are assumed also for M54, we need to add the same amount to $A(\text{Li})_0$ determined including efficient diffusion, thus obtaining $A(\text{Li})_0 \sim 2.45 \pm 0.11$ dex (or $A(\text{Li})_0 \sim 2.53 \pm 0.11$ dex when considering the NLTE corrections by Carlsson et al. 1994).

Given the current lack of identification of the proposed additional mixing with an established physical process, it is fair to say that we should be still cautious about this route to solve the cosmological Li problem, because simple parametric models have little predictive power. For example, to explain abundance trends in NGC 6397, NGC 6752 and M4 – and reconcile the measured $A(\text{Li})$ with $A(\text{Li})_{\text{BBN}}$ – one needs to employ a varying value of T_0 , generally increasing with increasing $[\text{Fe}/\text{H}]$. Whether or not this trend of T_0 with $[\text{Fe}/\text{H}]$ is a sign of the inadequacy of this parametrization of the additional mixing, requires a deeper understanding of its origin.

Observationally, NGC 6397 analysis by Gonzalez Hernandez et al. (2009), found a trend of the surface $A(\text{Li})$ with T_{eff} that is not explainable with the additional mixing of equation (1). Also, as discussed by Dobrovolskas et al. (2014), the constant Li abundance observed among the stars in Omega Centauri (Monaco et al. 2010) spanning a wide range of ages and metallicities, and the Li distribution observed in 47 Tuc seem to require fine-tuned mechanisms that are at present difficult to explain with simple parametric diffusive mixing prescriptions.

5 CONCLUSIONS

We measured the surface Li abundance in lower RGB stars harboured by M54, a GC belonging to the Sgr dwarf galaxy. We have obtained $A(\text{Li}) = 0.93 \pm 0.11$ dex, in agreement with measurements in Galactic halo stars. By considering the dilution due to the FDU, we have established an initial Li abundance of this stellar system ($A(\text{Li})_0 = 2.29 \pm 0.11$ and 2.35 ± 0.11 dex, without and with atomic diffusion, respectively) that is lower than the BBN value by ~ 0.3 dex. The cluster $A(\text{Li})_0$ can become compatible with $A(\text{Li})_{\text{BBN}}$ within $\sim 2\sigma$ only assuming diffusion plus the additional mixing prescriptions by Richard et al. (2005) calibrated on the (same metallicity) Galactic GC NGC 6752 (Gruyters et al. 2014). Alternatively, inadequacies of the BBN model used to derive $A(\text{Li})_{\text{BBN}}$ cannot be totally ruled out.

Also, an important question can be addressed by our study: Is the Li problem a *local* problem, limited to our Galaxy, or is it independent of the environment? The analysis of the RGB stars in M54 confirms the findings in ω Centauri (Monaco et al. 2010), considered as the remnant of an accreted dwarf galaxy: the Li problem seems to be a universal problem, regardless of the parent galaxy. The solution able to explain the discrepancy must work both in the Milky Way and other galaxies, with different origins and star formation histories. Thus, it seems unlikely that the scenario proposed by Piau et al. (2006), requiring that at least one-third of the Galactic halo has been processed by Population III, massive stars, can work in the same way also in smaller systems like Sgr and ω Centauri (see also Prantzos 2007). The universality of the *Spite plateau* and the lower RGB abundances is a constraint that must be satisfied by any theory aimed at solving the cosmological Li problem.

ACKNOWLEDGEMENTS

We warmly thank the referee, Andreas Korn, for his detailed comments that have helped to improve the paper significantly. SV gratefully acknowledges the support provided by Fondecyt reg. no. 1130721.

REFERENCES

- Alonso A., Arribas S., Martinez-Roger C., 1999, *A&AS*, 140, 261
Aoki W., Barklem P. S., Beers T. C., Christlieb N., Inoue S., Garca Pérez A. E., Norris J. E., Carollo D., 2009, *ApJ*, 698, 1803
Asplund M., Lambert D. L., Nissen P. E., Primas F., Smith V. V., 2006, *ApJ*, 644, 229
Bahcall J. N., Pinsonneault M. H., Basu S., Christensen-Dalsgaard J., 1997, *Phys. Rev. Lett.*, 78, 171
Bellazzini M. et al., 2008, *AJ*, 136, 1147
Boesgaard A. M., Deliyannis C. P., Stephens A., King J. R., 1998, 493, 206
Bonifacio P., 2002, *A&A*, 395, 515
Bonifacio P., Molaro P., 1997, *MNRAS*, 285, 847
Bonifacio P. et al., 2007, *A&A*, 462, 851
Carlsson M., Rutten R. J., Bruls J. H. M. J., Shchukina N. G., 1994, *A&A*, 288, 860
Carretta E. et al., 2010, *A&A*, 520, 95
Coc A., Uzan J.-P., Vangioni E., 2013, preprint ([arXiv:1307.6955](https://arxiv.org/abs/1307.6955))
Cyburt R. H., Fields B. D., Olive K. A., 2008, *J. Cosmol. Astropart. Phys.*, 11, 12
D’Orazi V., Lucatello S., Gratton R., Bragaglia A., Carretta E., Shen Z., Zaggia S., 2010, *ApJ*, 713, L1
D’Orazi V., Angelou G. C., Gratton R. G., Lattanzio J. C., Bragaglia A., Carretta E., Lucatello S., Momany Y., 2014, *ApJ*, 791, 39
Dobrovolskas V. et al., 2014, *A&A*, 565, 121
Gonzalez Hernandez J. I. et al., 2009, *A&A*, 505, L13
Gratton R. G., Carretta E., Eriksson K., Gustafsson B., 1999, *A&A*, 350, 955
Gratton R. G., Sneden C., Carretta E., Bragaglia A., 2000, *A&A*, 354, 169
Gratton R. G., Carretta E., Bragaglia A., 2012, *A&AR*, 20, 50
Gruyters P., Korn A. J., Richard O., Grundahl F., Collet R., Mashonkina L. I., Osorio Y., Barklem P. S., 2013, *A&A*, 555, 31
Gruyters P., Nordlander T., Korn A. J., 2014, *A&A*, 567, A72
Hinshaw G. et al., 2013, *ApJS*, 208, 19
Hosford A., Ryan S. G., Garcia Perez A. E., Norris J. E., Olive K. A., 2009, *A&A*, 493, 601
Iocco F., Mangano G., Miele G., Pisanti O., Serpico P. D., 2009, *Phys. Rep.*, 472, 1
Korn A. J., Grundahl F., Richard O., Barklem P. S., Mashonkina L., Collet R., Piskunov N., Gustafsson B., 2006, *Nature*, 442, 657
Layden A. C., Sarajedini A., 2000, *AJ*, 119, 1760
Lind K., Asplund M., Barklem P. S., Belyaev A. K., 2008, *A&A*, 528, 103
Lind K., Primas F., Charbonnel C., Grundahl F., Asplund M., 2009, *A&A*, 503, 545
Lind K., Asplund M., Barklem P. S., Belyaev A. K., 2011, *A&A*, 528, 103
McCall M. L., 2004, *AJ*, 128, 2144
Melendez J., Casagrande L., Ramirez I., Asplund M., Schuster W. J., 2010, *A&A*, 515, L3
Monaco L., Ferraro F. R., Bellazzini M., Pancino E., 2002, *ApJ*, 578, L47
Monaco L., Bellazzini M., Ferraro F. R., Pancino E., 2004, *MNRAS*, 353, 874
Monaco L., Bellazzini M., Ferraro F. R., Pancino E., 2005, *MNRAS*, 356, 1396
Monaco L., Bonifacio P., Sbordone L., Villanova S., Pancino E., 2010, *A&A*, 519, L3
Monaco L., Villanova S., Bonifacio P., Caffau E., Geisler D., Marconi G., Momany Y., Ludwig H.-G., 2012, *A&A*, 539, 157
Mucciarelli A., Salaris M., Lovisi L., Ferraro F. R., Lanzoni B., Lucatello S., Gratton R. G., 2011, *MNRAS*, 412, 81
Mucciarelli A., Salaris M., Bonifacio P., 2012, *MNRAS*, 419, 2195

- Mucciarelli A., Pancino E., Lovisi L., Ferraro F. R., Lapenna E., 2013, *ApJ*, 766, 78
- Nordlander T., Korn A. J., Richard O., Lind K., 2012, *ApJ*, 753, 48
- Pasquini L. et al., 2002, *The Messenger*, 110, 1
- Piau L., Beers T. C., Balsara D. S., Sivarani T., Truran J. W., Ferguson J. W., 2006, *ApJ*, 653, 300
- Pietrinferni A., Cassisi S., Salaris M., Castelli F., 2006, *ApJ*, 642, 797
- Planck Collaboration, 2013, preprint ([arXiv:1203.5076](https://arxiv.org/abs/1203.5076))
- Prantzos N., 2007, *Space Sci. Rev.*, 130, 27
- Rebolo R., Beckman J. E., Molaro P., 1988, *A&A*, 192, 192
- Richard O., Michaud G., Richer J., 2002, *ApJ*, 580, 1100
- Richard O., Michaud G., Richer J., 2005, *ApJ*, 619, 538
- Sbordone L., Bonifacio P., Castelli F., Kurucz R. L., 2004, *Mem. Soc. Astron. Ital. Suppl.*, 5, 93
- Shen Z.-X., Bonifacio P., Pasquini L., Zaggia S., 2010, *A&A*, 524, L2
- Siegel M. H. et al., 2007, *ApJ*, 667, L57
- Spergel D. N. et al., 2007, *ApJS*, 170, 377
- Spite M., Spite F., 1982, *Nature*, 297, 483
- Stetson P., Pancino E., 2008, *PASP*, 120, 1332
- Villanova S., Geisler D., 2011, *A&A*, 535, 31

This paper has been typeset from a $\text{\TeX}/\text{\LaTeX}$ file prepared by the author.